OPTICAL PROPERTIES OF PHOTONIC CRYSTAL FIBERS WITH A FIBER CORE OF ARRAYS OF SUB-WAVELENGTH CIRCULAR AIR HOLES: BIREFRIN-GENCE AND DISPERSION

D. Chen [†]

Institute of Information Optics
Zhejiang Normal University
Jinhua 321004, China

M.-L. V. Tse and H. Y. Tam

Photonics Research Centre
Department of Electrical Engineering
The Hong Kong Polytechnic University
Hung Hom, Kowloon, Hong Kong SAR, China

Abstract—We propose a kind of novel photonic crystal fibers (PCFs) based on a fiber core with arrays of subwavelength circular air holes, achieving the flexible control of the birefringence or the dispersion property of the PCFs. A highly birefringent (HB) PCF is achieved by employing arrays of subwavelength circular air hole pairs in the fiber core, which are arranged as a conventional hexagonal lattice structure with a subwavelength lattice constant. The HB-PCF is with uniform and ultrahigh birefringence (up to the order of 0.01) in a wavelength region from $1.25\,\mu$m to $1.75\,\mu$m or even a larger region, which, to the best of our knowledge, is the best birefringence property of the PCFs. A dispersion-flattened (DF) PCF with near-zero dispersion is achieved by employing arrays of subwavelength circular air holes in the fiber core arranged as a conventional hexagonal lattice structure with a subwavelength lattice constant, which contributes negative waveguide dispersion to the PCF. The proposed design of the DF-PCF provides an alternate approach for the dispersion control of the PCF. Besides the high birefringence and the flattened near-zero dispersion, the proposed PCFs with a fiber core of arrays of subwavelength circular air holes have the potential to achieve a large mode area single mode PCF.

Corresponding author: D. Chen (daru@zjnu.cn).
[†] Also with Photonics Research Centre, Department of Electrical Engineering, The Hong Kong Polytechnic University, Hung Hom, Kowloon, Hong Kong SAR, China.

1. INTRODUCTION

Thanks to the flexibility for the cross section design, photonic crystal fibers (PCFs) [1–9] have achieved excellent properties in birefringence [10–19], dispersion [20–29], single polarization single mode [30–32], nonlinearity [33], and effective mode area [34–36], and also excellent performances in the applications of fiber sensors [37, 38], fiber lasers [39–41] and nonlinear optics [42–45] over the past several years. Large numbers of research papers have highlighted some optical properties of the PCFs such as ultrahigh birefringence and unique chromatic dispersion, which are almost impossible for the conventional optical fibers. Optical fibers with high birefringence can find important applications in optical fiber communications, fiber filters, fiber sensors, fiber lasers and so on. So far, several highly birefringent (HB) PCFs have been demonstrated to achieve high birefringence up to the order of 0.001, which is one order of magnitude higher than that of the conventional polarization-maintaining fibers (PMFs). Most HB-PCFs are achieved based on the large index contrast of the silica and the air by introducing an asymmetric solid fiber core surrounded by air holes (e.g., using a fiber core with double defect or triple defect of the photonic crystal structure [12–15]). Several research papers have also shown that the ultrahigh birefringence (up to the order of 0.01) can be achieved by employing elliptical air holes in the fiber cladding [15–18]. For these so-called elliptical-hole PCFs, high birefringence is achieved when a large part of the mode power is in the fiber cladding. Thus, the high birefringence is often accompanied with poor light confinement (i.e., resulting in a large confinement loss). To overcome the problem of the poor light confinement of the elliptical-hole PCFs, we have proposed a PCF with both ultrahigh birefringence and ultralow confinement loss based on a fiber core with a structure of sub-wavelength elliptical air hole array [19]. However, it is almost impossible to accurately fabricate PCFs with different kinds of noncircular air holes (elliptical air holes) using the current fabrication techniques available. Moreover, compared with conventional optical fibers, PCFs have also shown their advantages in the control of chromatic dispersion which is very important for practical applications to optical communication systems, dispersion compensation, and nonlinear optics. Up to now, control techniques of the chromatic dispersion of PCFs are very attractive, and various PCFs with specific dispersion properties such as dispersion-flattened (DF) PCFs [22–25] and large negative dispersion PCFs [26–29] have been reported.

A PCF with a single subwavelength circular air hole in the fiber core has been reported [46], which indicates the large potential to

achieve PCFs with a relatively complex structure not only in the fiber cladding but also in the fiber core in the near future. In this paper, we proposed a kind of novel PCF based on the design of a fiber core with arrays of subwavelength circular air holes, at the same time, introducing approaches to achieve the ultrahigh birefringence and to control the dispersion property of PCFs. We investigate in detail two examples of the proposed PCFs, one HB-PCF design with arrays of subwavelength circular air hole pairs in the fiber core and one DF-PCF with arrays of subwavelength circular air holes in the fiber core. The proposed HB-PCF is with uniform and ultrahigh birefringence (up to the order of 0.01) which, to the best of our knowledge, is the best birefringence property of the any PCF designs, and is also with low confinement loss in a large wavelength region from $1.25\,\mu m$ to $1.75\,\mu m$ or even a larger region. By introducing the design of the DF-PCF with a zero dispersion wavelength around $1.55\,\mu m$, we also provide a dispersion control technique based on the negative waveguide dispersion property of the fundamental space-filling mode (FSM) of the fiber core with arrays of subwavelength circular air holes.

2. HIGHLY BIREFRINGENT PHOTONIC CRYSTAL FIBER

For a birefringent optical fiber, the modal birefringence is defined as [32]

$$\Delta n = n_{eff\text{-}y} - n_{eff\text{-}x}, \tag{1}$$

where $n_{eff\text{-}y}$ and $n_{eff\text{-}x}$ are effective indexes of the Y-polarized fundamental mode and X-polarized fundamental mode of the optical fiber, respectively. The confinement loss of the fundamental modes can be deduced from the value (imaginary part) of the complex effective index ($n_{eff\text{-}c}$) of the fundamental mode of the optical fiber, which is given by [11]

$$\alpha = 8.686 \times \text{Im}\left(\frac{2\pi}{\lambda} n_{eff\text{-}c}\right), \tag{2}$$

where λ is the operation wavelength. We employ a full-vector finite-element method (FEM) to calculate the effective index of the fundamental mode of the PCF in this paper.

Since the bulk fused silica is an isotropic medium, most HB-PCFs are achieved based on the asymmetric geometrical structure designs of the fiber core or the fiber cladding for the cross section of the PCFs. This leads to a difference in the effective indexes of the X-/Y-polarized guiding modes of PCFs. Quite different from the design principle of these HB-PCFs, here we design an equivalently anisotropic

medium [19] by employing subwavelength circular air hole pairs in the fused silica with a conventional hexagonal lattice structure, which intrinsically results in different effective indexes for the guiding light with different polarization. Since most mode power of the fundamental mode of the PCF locates in the fiber core, introducing the equivalently anisotropic medium in the fiber core can provide sufficient and flexible control of the birefringence of the PCF. In what follows we show an HB-PCF based on the new design concept.

Figure 1 shows the cross section of the proposed HB-PCF with a fiber core of subwavelength circular air hole pair array. Five rings of relatively large circular air holes with the radius (R) are employed in the fiber cladding forming a conventional hexagonal lattice structure with a lattice constant (Λ) (i.e., center-to-center distance between the two adjacent circular air holes). In the fiber core of the proposed HB-PCF, three rings of relatively small circular air hole pairs (including the central one) are also arranged in a hexagonal lattice but with a much shorter lattice constant (Λ'). Each circular air hole pair consists of two circular air holes with a distance (d) which are arranged in a line in Y-direction. The circular air holes in the fiber core are with the subwavelength size and the radius (r) is less than 100 nm for the HB-PCF considered in this paper. Note that the fiber core with arrays of the subwavelength circular air hole pairs in the fused silica acts as the equivalently anisotropic medium. We studied the HB-PCF by setting $\Lambda = 2\,\mu\text{m}$, $\Lambda' = 0.5\,\mu\text{m}$ and $d = 0.2\,\mu\text{m}$, and varied R and r. The refractive index of the air is assumed to be 1.0 and the refractive index of the fused silica is given by the following Sellmeier-type dispersion formula [47]

$$n^2 - 1 = \frac{0.6961663\lambda^2}{\lambda^2 - (0.0684043)^2} + \frac{0.4079426\lambda^2}{\lambda^2 - (0.1162414)^2} \frac{0.8974794\lambda^2}{\lambda^2 - (9.896161)^2} \quad (3)$$
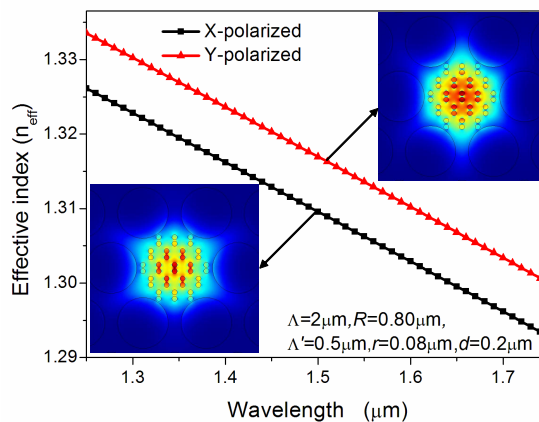
where the unit of λ is μm.

For the proposed HB-PCF with the parameters of $\Lambda = 2\,\mu\text{m}$, $R = 0.8\,\mu\text{m}$, $\Lambda' = 0.5\,\mu\text{m}$, $r = 0.08\,\mu\text{m}$ and $d = 0.2\,\mu\text{m}$, we calculated the
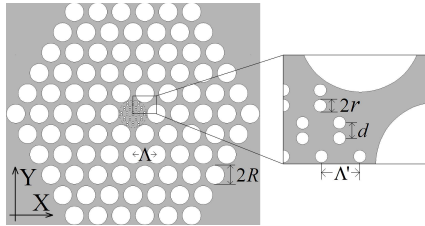
Figure 1. Cross section of the proposed HB-PCF with a fiber core of arrays of subwavelength circular air hole pairs.

effective index (n_{eff}, real part of $n_{eff\text{-}c}$) of the X-polarized fundamental mode and the Y-polarized fundamental mode of the HB-PCF in the wavelength region from $1.25\,\mu$m to $1.75\,\mu$m, which are shown in Figure 2 as black curve with rectangles and red curve with triangles, respectively. The effective index of the Y-polarized fundamental mode is much larger than that of the X-polarized fundamental mode for any wavelength from $1.25\,\mu$m to $1.75\,\mu$m. The large gap of the two effective index curves which are almost parallel with each other, indicates that the proposed HB-PCF exhibits uniform and ultrahigh birefringence as discussed hereinafter. Note that the effective index of the proposed HB-PCF became lower compared with the convetional PCF with a solid fiber core, because of the existence of the small air holes in the fiber core. Note for example, the effective index of the X- (Y-) polarized fundamental mode of the proposed HB-PCF is 1.3096 (1.3170) and the effective index of the PCF with a solid fiber core (but with the same parameters of $\Lambda = 2\,\mu$m, $R = 0.8\,\mu$m as the HB-PCF) is 1.3935 at the wavelength of $\lambda = 1.5\,\mu$m. The left bottom inset and the right top inset of Figure 2 show the electric field distributions of the X-polarized fundamental mode and the Y-polarized fundamental mode of the proposed HB-PCF at the wavelength of $\lambda = 1.5\,\mu$m, respectively. The mode area of the X-polarized fundamental mode and the Y-polarized
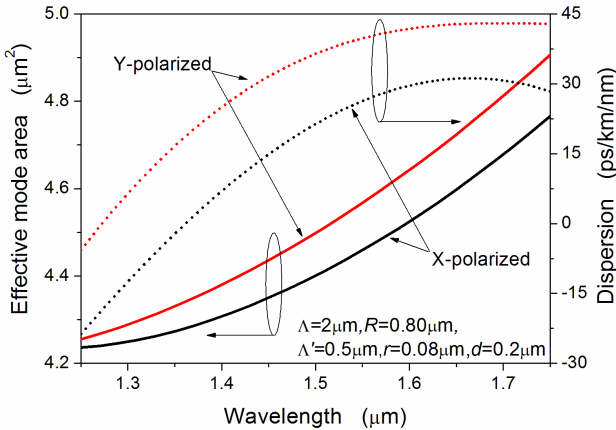

Figure 2. Effective index of the X-polarized and Y-polarized fundamental mode of the proposed HB-PCF with the parameters of $\Lambda = 2\,\mu$m, $R = 0.8\,\mu$m, $\Lambda' = 0.5\,\mu$m, $r = 0.08\,\mu$m and $d = 0.2\,\mu$m. Insets shows the electric field distributions of the X-polarized fundamental mode (left bottom) and the Y-polarized fundamental mode (right top) at the wavelength of $\lambda = 1.5\,\mu$m.

fundamental mode of the proposed HB-PCF is $A_{eff\text{-}x} = 4.4008\,\mu m^2$ and $A_{eff\text{-}y} = 4.4986\,\mu m^2$, respectively, corresponding to the mode area of $A_{eff} = 3.7968\,\mu m^2$ for the fundamental mode of the PCF with a solid fiber core at the wavelength of $\lambda = 1.5\,\mu m$. These results show that although the subwavelength air holes in the fiber core results in relatively low effective index, the HB-PCF has its fundamental mode profile just like the PCF with a solid fiber core. Figure 3 shows the effective mode area and the dispersion of the X-polarized and the Y-polarized fundamental modes of the proposed HB-PCF with the parameters of $\Lambda = 2\,\mu m$, $R = 0.8\,\mu m$, $\Lambda' = 0.5\,\mu m$, $r = 0.08\,\mu m$ and $d = 0.2\,\mu m$. The dispersion discussed here is the chromatic dispersion (including the waveguide dispersion and the material dispersion), which can be calculated by the following formula [11]

$$D = -\frac{\lambda}{c}\frac{\partial^2 n_{eff}}{\partial \lambda^2} \tag{4}$$

where c is the velocity of light in free space.

Next we investigated the birefringence property of the proposed HB-PCF. Figure 4 shows the birefringence of the proposed HB-PCFs in cases of ($R = 0.8\,\mu m$, $r = 0.08\,\mu m$, $d = 0.2\,\mu m$: black solid curve), ($R = 0.8\,\mu m$, $r = 0.09\,\mu m$, $d = 0.2\,\mu m$: red dotted curve), ($R = 0.75\,\mu m$, $r = 0.08\,\mu m$, $d = 0.2\,\mu m$: green dotted curve), and

Figure 3. Effective mode area and dispersion of the X-polarized and the Y-polarized fundamental modes of the proposed HB-PCF with the parameters of $\Lambda = 2\,\mu m$, $R = 0.8\,\mu m$, $\Lambda' = 0.5\,\mu m$, $r = 0.08\,\mu m$ and $d = 0.2\,\mu m$.
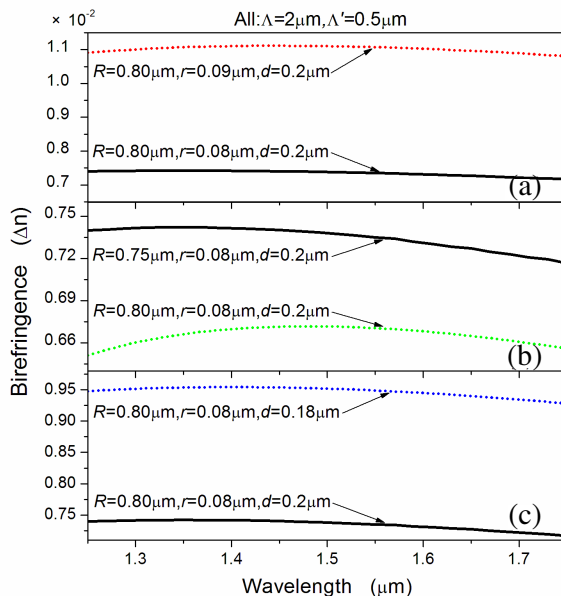
Figure 4. Birefringence of the proposed HB-PCFs in cases of ($R = 0.8\,\mu$m, $r = 0.08\,\mu$m, $d = 0.2\,\mu$m: black solid curve), ($R = 0.8\,\mu$m, $r = 0.09\,\mu$m, $d = 0.2\,\mu$m: red dotted curve), ($R = 0.75\,\mu$m, $r = 0.08\,\mu$m, $d = 0.2\,\mu$m: green dotted curve), and ($R = 0.8\,\mu$m, $r = 0.08\,\mu$m, $d = 0.18\,\mu$m: blue dotted curve). Note that other parameters of the HB-PCFs remain the same ($\Lambda = 2\,\mu$m and $\Lambda' = 0.5\,\mu$m).

($R = 0.8\,\mu$m, $r = 0.08\,\mu$m, $d = 0.18\,\mu$m: blue dotted curve). From Figure 4, the birefringence property of the proposed HB-PCF can be summarized as follows: 1) The birefringence of the proposed HB-PCF can reach a high level up to the order of 0.01. The perturbation of the birefringence in the calculated wavelength region is very small (within 3%), which shows the proposed HB-PCF exhibits uniform birefringence in the large wavelength region. 3) The birefringence increases as the size of the circular air hole in the fiber core increases, due to the enhancement of anisotropy of equivalently anisotropic medium in the fiber core. 4) The birefringence increases as the size of the circular air hole in the fiber cladding increases, due to the enhancement of light confinement (i.e., more mode power locates in the fiber core). 5) The birefringence depends on the distance (d) of the two subwavelength circular air holes of one pair. Figure 4(c) shows the birefringence increases as the distance (d) decreases. Our calculated results show

that the uniform and high birefringence property can be achieved based on our design and the proposed HB-PCF exhibits a flexible control of the birefringence by designing the structures of both the fiber cladding and the fiber core with suitable parameters.

It is also worthwhile to investigate the confinement loss property of the proposed HB-PCF. The confinement loss of the fundamental mode of the HB-PCF can be calculated by using Eq. (2). Figure 5 shows the confinement loss properties of the proposed HB-PCFs in cases of ($R = 0.8\,\mu\text{m}$, $r = 0.08\,\mu\text{m}$, $d = 0.2\,\mu\text{m}$: black curves), ($R = 0.8\,\mu\text{m}$, $r = 0.09\,\mu\text{m}$, $d = 0.2\,\mu\text{m}$: red curves), ($R = 0.75\,\mu\text{m}$, $r = 0.08\,\mu\text{m}$, $d = 0.2\,\mu\text{m}$: green curves), and ($R = 0.8\,\mu\text{m}$, $r = 0.08\,\mu\text{m}$, $d = 0.18\,\mu\text{m}$: blue curves). The HB-PCF with the parameters of ($R = 0.8\,\mu\text{m}$, $r = 0.08\,\mu\text{m}$, $d = 0.2\,\mu\text{m}$) exhibits low confinement loss (less than $0.03\,\text{dB/km}$ in the calculated wavelength region) which is much less than the propagating loss of the single mode fiber. The confinement
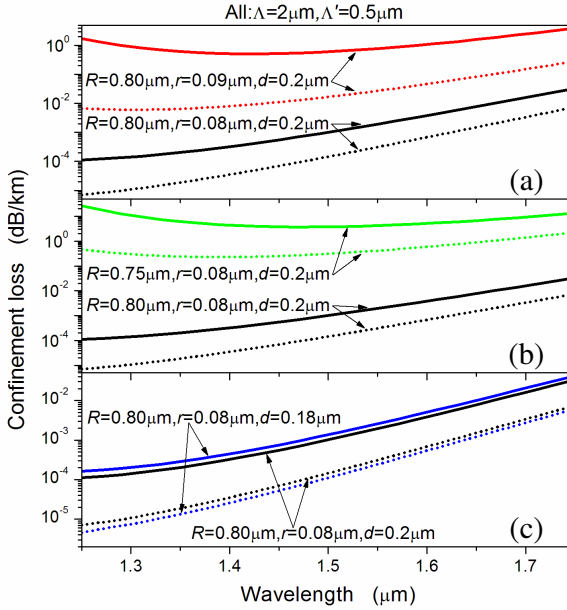

Figure 5. Confinement loss properties of the proposed HB-PCFs cases of ($R = 0.8\,\mu\text{m}$, $r = 0.08\,\mu\text{m}$, $d = 0.2\,\mu\text{m}$: black curves), ($R = 0.8\,\mu\text{m}$, $r = 0.09\,\mu\text{m}$, $d = 0.2\,\mu\text{m}$: red curves), ($R = 0.75\,\mu\text{m}$, $r = 0.08\,\mu\text{m}$, $d = 0.2\,\mu\text{m}$: green curves), and ($R = 0.8\,\mu\text{m}$, $r = 0.08\,\mu\text{m}$, $d = 0.18\,\mu\text{m}$: blue curves). Note that other parameters of the HB-PCFs remain the same ($\Lambda = 2\,\mu\text{m}$ and $\Lambda' = 0.5\,\mu\text{m}$).

loss of the HB-PCF with parameters of ($R = 0.8\,\mu$m, $r = 0.09\,\mu$m, $d = 0.2\,\mu$m) becomes larger since the larger circular air holes in the fiber core results in the lower effective index of the fiber core and more poor confinement of the guiding light. Similarly, the HB-PCF with parameters of ($R = 0.75\,\mu$m, $r = 0.08\,\mu$m, $d = 0.2\,\mu$m) also has the larger confinement loss due to the higher effective index of the fiber cladding because of the smaller circular air holes in the fiber cladding. The HB-PCF with the parameters of ($R = 0.8\,\mu$m, $r = 0.08\,\mu$m, $d = 0.18\,\mu$m) has the similar low confinement loss as the HB-PCF with the parameters of ($R = 0.8\,\mu$m, $r = 0.08\,\mu$m, $d = 0.2\,\mu$m) but has higher difference of the confinement loss for the X-polarized and the Y-polarized fundamental modes. Thus, one can conclude that the parameters of the circular air holes in the fiber cladding or the fiber core plays a critical role to control the effective index of the fiber cladding or the fiber core and consequently determine the confinement loss of the proposed HB-PCF, which provide flexibility to design or control the confinement loss of the proposed HB-PCF. We can also add more rings of circular air holes in the fiber cladding to further reduce the confinement loss, which will not affect the birefringence of the PCFs.

3. DISPERSION-FLATTENED PHOTONIC CRYSTAL FIBER

In the above section, we have shown that high birefringence can be achieved by employing the equivalently anisotropic medium formed by arrays of subwavelength circular air hole pairs in the fiber core. Naturally other property such as the dispersion of the PCF will also depend on the structure of the fiber core, since most mode power of the fundamental mode of the PCF locates in the fiber core. In this section, we will show the dispersion control technique of the PCF by introducing arrays of subwavelength circular air holes in the fiber core, where a DF-PCF is taken as an example.
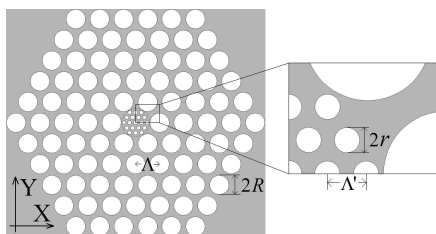

Figure 6. Cross section of the proposed DF-PCF with a fiber core of arrays of subwavelength air holes.

Figure 6 shows the cross section of the proposed DF-PCF with a fiber core of arrays of subwavelength circular air holes. The cross section of the DF-PCF is almost the same as that of the above-mentioned HB-PCF except that the fiber core of the DF-PCF is formed by arrays of the subwavelength circular air holes instead of the subwavelength circular air hole pairs. Note that the fiber core of the DF-PCF with arrays of subwavelength circular air holes in the fused silica acts as the equivalently isotropic medium here, which indicates the birefringence of the DF-PCF is almost zero and will not be discussed in this section. For the ease of calculation, we have set $\Lambda = 2\,\mu\text{m}$, $R = 0.8\,\mu\text{m}$ and $\Lambda' = 0.5\,\mu\text{m}$. Different values of the radius (r) of the circular air holes in the fiber core are considered in this section to show the dispersion contribution of the fiber core structure. The refractive index of the air also is assumed to be 1.0 and the refractive index of the fused silica is given by the Eq. (3), which means material dispersion is also included in our calculations.

First, we investigated the waveguide dispersion of the hexagonal lattice structure with arrays of circular air holes in the fused silica. This helped us to understand what role the fiber core of the DF-PCF plays for the dispersion property of the DF-PCF. A plane-wave expansion method [48] is used to calculate the effective indexes for the light wave propagating along the Z-direction in the fiber core area of the DF-PCF with the hexagonal lattice structure (i.e., the effective indexes of the fundamental space-filling mode (FSM) of the fiber core). The lattice constant and the radius of the air hole are assumed to be $\Lambda' = 1\,\mu\text{m}$ and $r = 0.25\,\mu\text{m}$, respectively. The refractive index of the fused silica is fixed to be 1.45 here, since we only consider the waveguide dispersion of the structure. Figure 7 shows calculated effective refractive index as a function of wavelength for the hexagonal lattice structure in a wavelength region from 0 to $2.2\,\mu\text{m}$. The effective index curve can be separated into two sections in two wavelength regions of [0–0.485 μm] and [0.485 μm–2.2 μm], corresponding to a convex function and a concave function, respectively. According to Eq. (4) we can calculate the dispersion as shown in the inset of the Figure 7, where positive dispersion and negative dispersion are found in the wavelength regions of [0–0.485 μm] and [0.485 μm–2.2 μm], respectively. Thus, we know the fiber core of the present DF-PCF with arrays of the subwavelength circular air holes will contribute negative dispersion for the PCF when only waveguide dispersion of the fiber core is considered.

Figure 8(a) shows the effective index of three types of PCFs, Type-I PCF with a solid fiber without air hole (black solid curve), Type-II PCF with a fiber core with arrays of circular air holes of $\Lambda' = 0.5\,\mu\text{m}$ and $r = 0.1\,\mu\text{m}$ (red dashed curve), and Type-III PCF
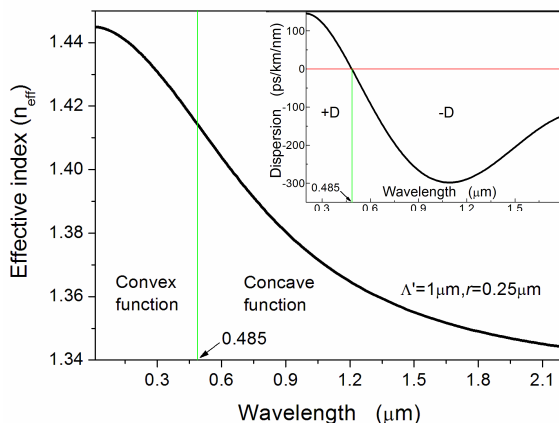
Figure 7. Calculated effective index (as a function of wavelength) for the hexagonal lattice structure (i.e., the FSM of the fiber core) of $\Lambda' = 1\,\mu m$ and $r = 0.25\,\mu m$. Inset shows the calculated dispersion of the FSM of the hexagonal lattice structure. Note that the effective index is a convex function (corresponding to positive dispersion) or a concave function (corresponding to negative dispersion) versus wavelength in the wavelength regions of $[0$–$0.485\,\mu m]$ or $[0.485\,\mu m$–$2.2\,\mu m]$.

with a fiber core with arrays of circular air holes of $\Lambda' = 0.5\,\mu m$ and $r = 0.12\,\mu m$ (green dotted curve). Figure 8(b) shows the dispersion of the fundamental modes of Type-I PCF (black solid curve), Type-II PCF (red dashed curve), Type-III PCF (green dotted curve), and the FSMs of the hexagonal lattice structures in cases of ($\Lambda' = 0.5\,\mu m$, $r = 0.1\,\mu m$) (yellow dotted curve) and ($\Lambda' = 0.5\,\mu m$, $r = 0.12\,\mu m$) (blue dashed curve). Note that the dispersion of FSMs of the hexagonal lattice structures is calculated by employing the plane-wave expansion method and the fused silica is assumed to be 1.45. Type-I PCF is actually a conventional PCF with the positive dispersion in the calculated wavelength region, which includes the waveguide dispersion due to the cross section structure and the material dispersion of the fused silica. When arrays of the subwavelength circular air holes are introduced in the fiber core, the dispersion of the PCFs (such as Type-II PCF and Type-III PCF) is reduced due to the fact that the hexagonal lattice structure with arrays of the subwavelength circular air holes in the fused silica have the negative waveguide dispersion as discussed above. Since the negative waveguide dispersion of the hexagonal lattice structure in the fiber core can be designed by choosing suitable parameters of the air hole size and the lattice constant, the

dispersion property of the PCF can be flexibly controlled and the flattened near-zero dispersion can be achieved. Type-III PCF is a DF-PCF with flattened dispersion in the wavelength region from 1.5 μm to
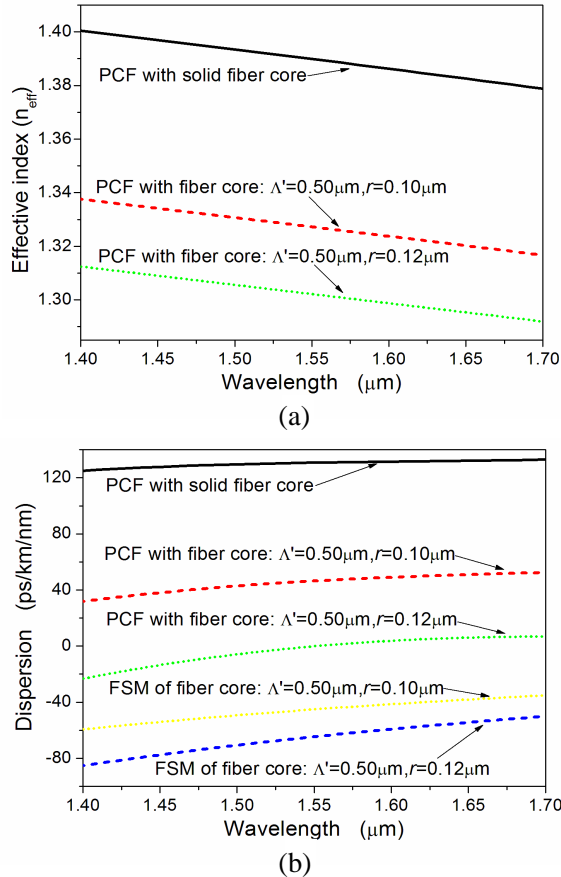
Figure 8. (a) Effective index of the fundamental modes of the PCF with a solid fiber core (black solid curve), the PCF with a fiber core in case of ($\Lambda' = 0.5\,\mu\text{m}$, $r = 0.1\,\mu\text{m}$) (red dashed curve) and the PCF with a fiber core in case of ($\Lambda' = 0.5\,\mu\text{m}$, $r = 0.12\,\mu\text{m}$) (green dotted curve). (b) Dispersion of the fundamental modes of the PCF with solid fiber core (black solid curve), the PCF with a fiber core in case of ($\Lambda' = 0.5\,\mu\text{m}$, $r = 0.1\,\mu\text{m}$) (red dashed curve) and the PCF with a fiber core in case of ($\Lambda' = 0.5\,\mu\text{m}$, $r = 0.12\,\mu\text{m}$) (green dotted curve) and the FSMs of the fiber cores in cases of ($\Lambda' = 0.5\,\mu\text{m}$, $r = 0.1\,\mu\text{m}$) (yellow dotted curve) and ($\Lambda' = 0.5\,\mu\text{m}$, $r = 0.12\,\mu\text{m}$) (blue dashed curve).
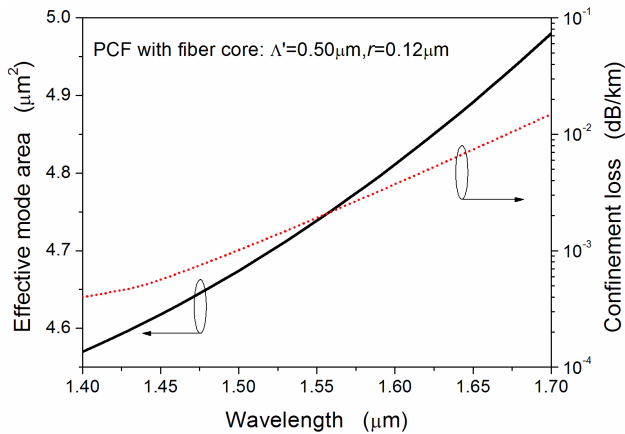
Figure 9. Effective mode area and confinement loss of the fundamental modes of the PCF with a fiber core in case of ($\Lambda' = 0.5\,\mu\text{m}$, $r = 0.12\,\mu\text{m}$).

$1.6\,\mu\text{m}$ (the fiber optical communication window) and a zero-dispersion wavelength around $1.55\,\mu\text{m}$. Figure 9 shows the effective mode area and the confinement loss of the fundamental modes of the PCF with a fiber core in case of ($\Lambda' = 0.5\,\mu\text{m}$, $r = 0.12\,\mu\text{m}$), where the confinement loss is very low in the calculated wavelength region.

4. DISCUSSION AND CONCLUSION

It is well known that PCFs' excellent properties in birefringence, dispersion, nonlinearity, and effective mode area are mainly due to the flexibility for the cross section design. *Knight* has concluded there are four types of PCFs which are with solid fiber cores (silica) or hollow fiber cores (air) [5]. So far, most designs for PCFs are focusing on the fiber cladding structure. In general, we introduce the designs of PCFs with fiber cores of relative complex structure, which provide additional degree of freedom for PCF designs to achieve excellent properties such as high birefringence, flattened dispersion or large effective mode area where the former two have been demonstrated in this paper. For the HB-PCF, we employ arrays of subwavelength circular air hole pairs in the fiber core which acts as equivalently anisotropic medium and result in uniform and ultrahigh birefringence. The equivalently anisotropic medium is mainly due to the effect of the two Y-direction-arranged circular air holes which form the basic cell of the air hole pair. Similarly, as shown in Figure 10 we can also use three air holes or four air holes
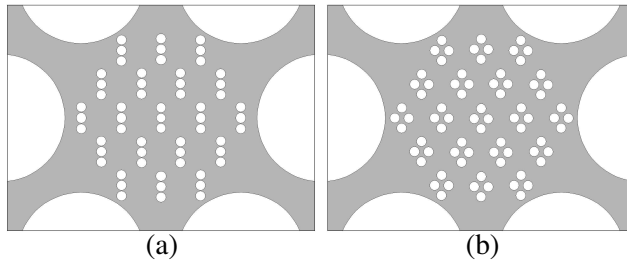
Figure 10. Cross sections of the fiber core of HB-PCFs based on (a) three-hole super-lattice structure and (b) four-hole super-lattice structure.

to form the basic cell of the structure in the fiber core to introduce high birefringence of the PCF, which benefit from the design concept of super-lattice structure in our recent paper [49]. Note that we can also use X-direction-arranged circular air holes in the fiber core to achieve the HB-PCF. For the DF-PCF, we observe that the waveguide dispersion of the fiber core structure plays an important role in the dispersion of the PCF. Thus, the fiber core structure design provides an additional approach to control the dispersion of the PCF. Besides the method we adjust the size of the subwavelength air hole in the fiber core to achieve the dispersion control, we can also adjust the hole pitch of the subwavelength air hole in the fiber core or the size of the big air hole in the fiber cladding of the PCF. It is worthwhile to note that the effective index of the fiber core can be flexibly controlled by adjusting the parameters such as the hole size in the fiber core, which indicates the index difference between the fiber core and the fiber cladding can be well controlled. This is extremely important for a single mode design and a large mode area design of the PCFs. By employing arrays of subwavelength air holes with suitable parameters in the fiber core of the PCF we can achieve very small difference between the effective indexes of the fiber core and the fiber cladding, which allows a vary large diameter of the fiber core when consider the single mode condition. Thus, the proposed design by employing arrays of subwavelength circular air holes in the fiber core has a big potential to achieve a large mode area single mode PCF.

For the proposed PCFs with a fiber core of arrays of subwavelength circular air holes, excellent properties in the birefringence and the dispersion are introduced due to the fact that most mode power locates in the fiber core region. As shown in Figure 11(a), it is better to design a large fiber core region (red part) which ensures that most mode power locates in the fiber core region with arrays of subwavelength
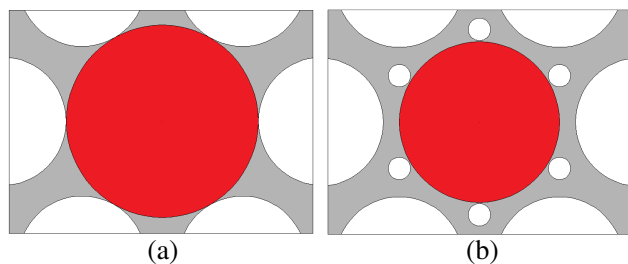
Figure 11. Cross sections of PCFs with (a) a large fiber core region (red part) and (b) a small fiber core region (red part).

circular air holes. Otherwise, expected property of the PCFs such as the high birefringence can not be achieved when large part of the mode power locates in the uniform fusa silica region (outside of the fiber core region). Considering the proposed PCFs may not be easily produced by the traditional stacking of capillaries method, as a large fiber core region is required, another alternative is to have a smaller fiber core region and 6 additional air holes between the core and cladding region as shown in Figure 11(b). The 6 air holes ensured most of the mode power confined within the fiber core region. For all PCF designs in this paper, a secondary (or even third) stacking of canes method should be employed in the fabrication process, where the fiber core with arrays of subwavelength air holes should be fabricated in the first (or second) stacking of canes.

Introducing arrays of subwavelength circular air holes in the fiber core of the PCF is a creative and challenging idea. Although the proposed PCFs have very low confinement loss, they may have other problems such as the scattering loss because of the small air holes in the fiber core and the coarse interfaces between the air and the silica, which will depend on the technological level of the PCF fabrication. Due to the excellent properties of the proposed PCFs, it is worthwhile to try to fabricate them and to check whether they work well for many of the applications of the HB-PCF and the DF-PCF, which are usually with a length less than tens of meters for specific applications [39, 41].

In conclusion, we have proposed a kind of novel PCFs based on a fiber with arrays of subwavelength circular air holes, which include an HB-PCF and a DF-PCF. For the HB-PCF with arrays of subwavelength circular air hole pairs in the fiber core, uniform and ultrahigh birefringence in a large wavelength region has been achieved. Simulation results have also shown that the birefringence is dependent on the size of the air holes in the fiber core and the fiber cladding. For the DF-PCF with arrays of subwavelength circular air holes in the

fiber core, fattened near-zero dispersion is achieved where the negative waveguide dispersion of the fiber core structure is introduced. We have also investigated the waveguide dispersion of the hexagonal lattice structure with arrays of circular air holes in the fused silica. Simulation results have shown that the designs of the fiber core with arrays of circular air holes can provide an additional approach for the dispersion control of the PCF.

ACKNOWLEDGMENT

REFERENCES

1. Knight, J. C., T. A. Birks, P. S. J. Russell, and D. M. Atkin, "All-silica single-mode optical fiber with photonic crystal cladding," *Opt. Lett.*, Vol. 21, 1547–1549, 1996.

2. Birks, T. A., J. C. Knight, and P. S. J. Russel, "Endlessly single-mode photonic crystal fiber," *Opt. Lett.*, Vol. 22, 961–963, 1997.

3. Knight, J. C., J. Broeng, T. A. Birks, and P. S. J. Russell, "Photonic band gap guidance in optical fibers," *Science*, Vol. 282, 1476–1478, 1998.

4. Knight, J. C. and P. S. J. Russell, "Photonic crystal fibers: New way to guide light," *Science*, Vol. 296, 276–277, 2002.

5. Knight, J. C. "Photonic crystal fibers," *Nature*, Vol. 424, 847–851, 2003.

6. Shen G.-F., X.-M. Zhang, H. Chi, and X.-F. Jin, "Microwave/millimeter-wave generation using multi-wavelength photonic crystal fiber brillouin laser," *Progress In Electromagnetics Research*, Vol. 80, 307–320, 2008.

7. Nozhat N. and N. Granpayeh, "Specialty fibers designed by photonic crystals," *Progress In Electromagnetics Research*, Vol. 99, 225–244, 2009.

8. Wu J.-J., D. Chen, K.-L. Liao, T.-J. Yang, and W.-L. Ouyang, "The optical properties of bragg fiber with a fiber core of 2-dimension elliptical-hole photonic crystal structure," *Progress In Electromagnetics Research Letters*, Vol. 10, 87–95, 2009.

9. Chau Y.-F., C.-Y. Liu, H.-H. Yeh, and D. P. Tsai, "A comparative study of high birefringence and low confinement loss photonic

crystal fiber employing elliptical air holes in fiber cladding with tetragonal lattice," *Progress In Electromagnetics Research B*, Vol. 22, 39–52, 2010.

10. Ortigosa-Blanch, A., J. C. Knight, W. J. Wadsworth, J. Arriaga, B. J. Mangan, T. A. Birks, and P. S. J. Russel, "Highly birefringent photonic crystal fibers," *Opt. Lett.*, Vol. 25, 1325–1327, 2000.

11. Ademgil, H. and S. Haxha, "Highly birefringent photonic crystal fibers with ultralow chromatic dispersion and low confinement losses," *J. Lightwave Technol.*, Vol. 26, 441–448, 2008.

12. Hansen, T. P., J. Broeng, S. E. B. Libori, E. Knudsen, A. Bjarklev, J. R. Jensen, and H. Simonsen, "Highly birefringent index-guiding photonic crystal fibers," *IEEE Photon. Technol. Lett.*, Vol. 13, 588–590, 2001.

13. Sapulak, M., G. Statkiewicz, J. Olszewski, T. Martynkien, W. Urbanczyk, J. Wojcik, M. Makara, J. Klimek, T. Nasilowski, F. Berghmans, and H. Thienpont, "Experimental and theoretical investigations of birefringent holey fibers with a triple defect," *Appl. Opt.*, Vol. 44, 2652–2658, 2005.

14. Anthkowiak, M., R. Kotynski, T. Nasilowski, P. Lesiak, J. Wojcik, W. Urbanczyk, F. Berghmans, and H. Thienpont, "Phase and group modal birefringence of triple-defect photonic crystal fibres," *J. Opt. A: Pure Appl. Opt.*, Vol. 7, 763–766, 2005.

15. Chen, D. and L. Shen, "Highly birefringent elliptical-hole photonic crystal fibers with double defect," *J. Lightw. Technol.*, Vol. 25, 2700–2705, 2007.

16. Steel, M. J. and R. M. Osgood, "Elliptical-hole photonic crystal fibers," *Opt. Lett.*, Vol. 26, 229–231, 2001.

17. Steel, M. J. and R. M. Osgood, "Polarization and dispersive properties of elliptical-hole photonics crystal fibers," *J. Lightwave Technol.*, Vol. 19, 495–503, 2001.

18. Yue, Y., G. Kai, Z. Wang, T. Sun, L. Jin, Y. Lu, C. Zhang, J. Liu, Y. Li, Y. Liu, S. Yuan, and X. Dong, "Highly birefringent elliptical-hole photonic crystal fiber with squeezed hexagonal lattice," *Opt. Lett.*, Vol. 32, 469–471, 2007.

19. Chen, D. and L. Shen, "Ultrahigh birefringent photonic crystal fiber with ultralow confinement loss," *IEEE Photon. Technol. Lett.*, Vol. 19, 185–187, 2007.

20. Agrawal, A., N. Kejalakshmy, J. Chen, B. M. A. Rahman, and K. T. V. Grattan, "Golden spiral photonic crystal fiber: Polarization and dispersion properties," *Opt. Lett.*, Vol. 33, 2716–

2718, 2008.

21. Shen, L. P., W. P. Huang, and S. S. Jian, "Design of photonic crystal fibers for dispersion-related applications," *J. Lightwave Technol.*, Vol. 21, 1644–1651, 2003.

22. Ferrando, A., E. Silvestre, J. J. Miret, and P. Andres, "Nearly zero ultraflattened dispersion in photonic crystal fibers," *Opt. Lett.*, Vol. 25, 790–792, 2000.

23. Ferrando, A., E. Silvestre, P. Andres, J. Miret, and M. Andres, "Designing the properties of dispersion-flattened photonic crystal fibers," *Opt. Express*, Vol. 9, 687–697, 2001.

24. Saitoh, K., M. Koshiba, T. Hasegawa, and E. Sasaoka, "Chromatic dispersion control in photonic crystal fibers: Application to ultra-flattened dispersion," *Opt. Express*, Vol. 11, 843-852, 2003.

25. Poletti F., V. Finazzi, T. M. Monro, N. G. R. Broderick, V. Tse, and D. J. Richardson, "Inverse design and fabrication tolerances of ultra-flattened dispersion holey fibers," *Opt. Express*, Vol. 13, 3728–3736, 2005.

26. Gérôme, F., J.-L. Auguste, and J.-M. Blondy, "Design of dispersion-compensating fibers based on a dual-concentric-core photonic crystal fiber," *Opt. Lett.*, Vol. 29, 2725–2727, 2004.

27. Huttunen, A. and P. Törmä, "Optimization of dual-core and microstructure fiber geometries for dispersion compensation and large mode area," *Opt. Express*, Vol. 13, 627–635, 2005.

28. Varshney, S. K., T. Fujisawa, K. Saitoh, and M. Koshiba, "Design and analysis of a broadband dispersion compensating photonic crystal fiber Raman amplifier operating in S-band," *Opt. Express*, Vol. 14, 3528–3540, 2006.

29. Yang, S., Y. Zhang, X. Peng, Y. Lu, S. Xie, J. Li, W. Chen, Z. Jiang, J. Peng, and H. Li, "Theoretical study and experimental fabrication of high negative dispersion photonic crystal fiber with large area mode field," *Opt. Express*, Vol. 14, 3015–3023, 2006.

30. Ju, J., W. Jin, and M. S. Demokan, "Design of single-polarization single mode photonics crystal fibers," *J. Lightwave Technol.*, Vol. 24, 825–830, 2001.

31. Saitoh, K. and M. Koshiba, "Single-polarization single-mode photonic crystal fibers," *IEEE Photon. Technol. Lett.*, Vol. 15, 1384–1340, 2003.

32. Kubota, H., S. Kawanishi, S. Koyanagi, M. Tanaka, and S. Yamaguchi, "Absolutely single polarization photonic crystal fiber," *IEEE Photon. Technol. Lett.*, Vol. 16, 182–184, 2004.

33. Knight, J. C. and D. V. Skryabin, "Nonlinear waveguide optics

and photonic crystal fibers," *Opt. Express*, Vol. 15, 15365–15376, 2007.

34. Mortensen, N. A., M. D. Nielsen, J. R. Folkenberg, A. Petersson, and H. R. Simonsen, "Improved large-mode-area endlessly single-mode photonic crystal fibers," *Opt. Lett.*, Vol. 28, 393–395, 2003.

35. Limpert, J., T. Schreiber, S. Nolte, H. Zellmer, T. Tunnermann, R. Iliew, F. Lederer, J. Broeng, G. Vienne, A. Petersson, and C. Jakobsen, "High-power air-clad large-mode-area photonic crystal fiber laser," *Opt. Express*, Vol. 11, 818–823, 2003.

36. Folkenberg, J., M. Nielsen, N. Mortensen, C. Jakobsen, and H. Simonsen, "Polarization maintaining large mode area photonic crystal fiber," *Opt. Express*, Vol. 12, 956–960, 2004.

37. Dobb, H., K. Kalli, and D. J. Webb, "Temperature-insensitive long period grating sensors in photonic crystal fibre," *Eletron. Lett.*, Vol. 40, 657–658, 2004.

38. Dong, X. and H. Y. Tam, "Temperature-insensitive strain sensor with polarization-maintaining photonic crystal fiber based on Sagnac interferometer," *Appl. Phys. Lett.*, Vol. 90, 151113, 2007.

39. Wadsworth, W. J., J. C. Knight, W. H. Reewes, P. S. J. Russell, and J. Arriaga, "Yb^{3+}-doped photonic crystal fibre laser," *Eletron. Lett.*, Vol. 36, 1452–1253, 2000.

40. Liu, X., X. Zhou, X. Tang, J. Ng, J. Hao, T. Chai, E. Leong, and C. Lu, "Swithable and tunable multiwavelength erbium-doped fiber laser with fiber Bragg grating and photonic crystal fiber," *IEEE Photon. Technol. Lett.*, Vol. 17, 1626–1628, 2005.

41. Chen, D., "Stable multi-wavelength erbium-doped fiber laser based on photonic crystal fiber Sagnac loop filter," *Laser Phys. Lett.*, Vol. 4, 437–439, 2007.

42. Broderick, N. G. R., T. M. Monro, P. J. Bennett, and D. J. Richardson, "Nonlinearity in holey optical fibers: Measurement and future opportunities," *Opt. Lett.*, Vol. 24, 1395–1397, 1999.

43. Zhu, Z. and T. G. Brown, "Experimental studies of polarization properties of supercontinua generated in a birefringent photonic crystal fiber," *Opt. Express*, Vol. 12, 791–796, 2004.

44. Zhu, Z. and T. G. Brown, "Polarization properties of supercontinuum spectra generated in birefringent photonic crystal fibers," *J. Opt. Soc. Am. B*, Vol. 21, 249–257, 2004.

45. Dudley, J. M. and J. R. Taylor, "Ten years of nonlinear optics in photonic crystal fibre," *Nature Photonics*, Vol. 3, 85–90, 2009.

46. Wiederhecher, G. S., C. M. B. Cordeiro, F. Couny, F. Benabid,

S. A. Maier, J. C. Knight, C. H. B. Cruz, and H. L. Fragnito, "Field enhancement within an optical fibre with a subwavelength air core," *Nature Photonics*, Vol. 1, 115–118, 2007.

47. Klocek, P., *Handbook of Infrared Optical Materials*, Marcel Dekker, New York, NY, 1991.

48. Meade, R. D., A. M. Rappe, K. D. Brommer, J. D. Joannopoulos, and O. L. Alerhand, "Accurate theoretical analysis of photonic band-gap matetrials," *Phys. Rev. B*, Vol. 48, 8434–8437, 1993.

49. Chen, D., M.-L. Vincent Tse, and H. Y. Tam, "Super-lattice structure photonic crystal fiber," *Progress In Electromagnetics Research M*, Vol. 11, 53–64, 2010.